Supporting Information

Leemburg et al. 10.1073/pnas.1002570107

SI Materials and Methods

Animals and Surgical Procedures. Male Wistar Kyoto rats (3–4 mo, 250–350 g; Charles River) were maintained on a 12:12 light–dark cycle (lights on at 10:00 AM; room temperature 23 ± 1 °C), with food and water available ad libitum for the duration of the experiment. For electroencephalographic (EEG) recordings rats were implanted bilaterally with epidural screw electrodes over the frontal (anteroposterior, AP, +2.5 mm from bregma; mediolateral, ML, 3 mm), parietal (AP −2.5 mm; ML 5 mm), and occipital (AP −7 mm; ML 3.5 mm) cortex. Ground and reference electrodes were implanted over the cerebellum. Two stainless steel wires inserted into the neck muscles served as electromyogram (EMG) electrodes. After surgery, rats were allowed to recover in individual Plexiglas cages (36.5 × 25 × 46 cm) for at least 2 d before they were transferred to the disk (see below). For the final EEG analysis the "best" electrode (most stable signal throughout the experiment, lowest number of artifacts) for each cortical area was selected in each rat (left hemisphere: frontal, $n = 6$, parietal, $n = 5$, occipital, $n = 6$; right hemisphere: frontal, $n = 5$, parietal, $n = 6$, occipital, $n = 5$). All animal procedures followed the National Institutes of Health Guide for the Care and Use of Laboratory Animals and facilities were reviewed and approved by the Institutional Animal Care and Use Committee of the University of Wisconsin-Madison.

Sleep Restriction (SR). Twenty hours of SR ($20S^-$) were enforced using the disk-over-water (DOW) method, a well-established technique for long-term sleep deprivation (1). The rat is placed on one-half of a rotating platform (18 in in diameter) located above a tray filled with water. When the DOW rotates the rat must keep moving to avoid falling into the water. After recovery from surgery rats were transferred to the DOW, which remained stationary for several days, then was continuously rotated for 15 min immediately after light onset for 3–4 d to habituate the animals to the movement. The experiments began only after all rats were well adapted to this procedure and their sleep–wake cycle had fully normalized (see below, baseline sleep on the DOW; Fig. S1). A 24-h baseline was then recorded, followed by 5 d of SR. During SR the DOW was stationary for the first 4 h after light onset, allowing undisturbed sleep ($4S^+$) and rotated during $20S^-$, preventing consolidated periods of sleep. SR was followed by 2 d of undisturbed recovery on the stationary DOW.

We tested different protocols of DOW rotation (0.6 or 2 rpm with random change in direction every 20 s; 2.5 rpm with no change in direction) and found that their effectiveness in preventing sleep was similar, but suboptimal. Indeed, we soon realized from online EEG observation that sleep could be almost completely prevented only if there was constant monitoring by the experimenter during $20S^-$. This was needed to quickly repair the DOW if it stopped working, and, more importantly, to anticipate any attempt by the rat to go to sleep even for just a few seconds by introducing novel objects. Moreover, we found that several rats, if left alone, adopted strategies that allowed them to sleep on the rotating DOW without falling off. In these cases, objects were hung from the cage walls to distract the animal or physically impede their strategy. During repairs, rats were placed in cages with clean bedding, food, and novel objects. EEG and EMG were still continuously recorded and monitored during these periods. To assure that the animals had sufficient time for eating, drinking, and grooming the DOW was stopped every few hours for 10–15 min under the supervision of the experimenter. The DOW was also stopped for cleaning for 10–15 min before 10 AM, to allow undisturbed recovery immediately at light onset. Daily monitoring of the animals' physical appearance did not find obvious signs of discomfort or debilitation. A small weight loss (~10% by the end of the experiment) occurred in a few animals.

Scoring of Vigilance States. During baseline, NREM sleep, REM sleep, and wake were scored offline by visual inspection of 4-s epochs (SleepSign; Kissei Comtec) according to standard criteria (Fig. S5*A*). Three EEG signals (frontal, parietal, and occipital) and the EMG were used for scoring. Wake was characterized by low voltage, high frequency EEG pattern and phasic EMG activity. NREM sleep was characterized by the occurrence of high amplitude slow waves, spindles, and low tonic EMG activity. The EEG during REM sleep resembled that of wake, but only heartbeats and occasional twitches were present in the EMG signal. Since one of the main goals of the study was to assess the effects of SR on the wake EEG, we took extreme care in excluding from the latter even very short episodes containing slow waves. Thus, although according to standard scoring rules a 4-s epoch containing <2 s of slow waves would still be counted as "wake," we used a more conservative approach. Specifically, epochs were scored as NREM sleep when the amplitude of the EEG was at any point during the 4 s increased more than 2-fold compared with the typical levels observed during wake EEG. This occurred due to the sporadic (1–1.5 s) occurrence of slow waves similar to those typical of NREM sleep (e.g., Fig. S5*B*). Isolated slow waves (<2 s) were also sometimes present in REM sleep during $4S^+$ and recovery, but such cases were not considered an interruption of REM sleep unless a clearcut transition to NREM sleep was apparent, i.e., the slow waves comprised more than half of the epoch and were present also in the following epochs.

Behavioral observation revealed that epochs with increased SWA during $20S^-$ were often associated with immobility and an attempt to assume a sleep-like posture. Such episodes were considered sleep attempts if they were <20 s and were preceded and followed by wake episodes >20 s (Fig. S5*C*). NREM sleep episodes instead were defined as periods of NREM sleep lasting >16 s, preceded or followed by wake or REM sleep (2–4). Brief awakenings (5) were defined as short episodes of arousal, characterized by flattening of the EEG signal in all three derivations and concomitant increase of the EMG tone lasting ≤16 s and preceded and followed by NREM sleep. Sleep latency was defined as the time elapsed between the beginning of the $4S^+$ period and the first NREM sleep episode lasting >16 s.

During offline scoring the epochs with movement or technical artifacts were carefully marked to be excluded from spectral analysis. The absence of artifacts was verified post hoc on each individual 24-h profile of SWA in each derivation. During baseline, only 4.6 ± 1.2% of all epochs were scored as artifacts (95.6 ± 1.3% of them occurred during wake), and during SR the number was only marginally higher (5.9 ± 1.6%, 96.7 ± 1.5% in wake). Three rats in which one or more EEG channels showed deterioration during the experiment (overall decrease in total EEG power and signal amplitude >20%) were excluded from spectral analysis but included in the analysis of vigilance states, since the latter could still be reliably determined.

Signal Processing and Analysis. Data acquisition was performed with the Multichannel Neurophysiology Recording System (Tucker-Davis Technologies, TDT). EEG and EMG were collected continuously at a sampling rate of 256 Hz (filtered between 0.1–100 Hz). For staging, signals were loaded in custom-made Matlab

programs using standard TDT routines, and subsequently transformed into the European Data Format (EDF) with Neurotraces software (www.neurotraces.com). Video recordings were performed continuously with infrared cameras and stored in real time. EEG power spectra were computed by a fast Fourier transform (FFT) routine for 4-s epochs (SleepSign, Kissei, 0.25-Hz resolution).

Detection of individual slow waves was performed on the EEG signal after band pass filtering (0.5–4 Hz, stopband edge frequencies 0.1–10 Hz) with MATLAB filtfilt function exploiting a Chebyshev type II filter design (MATLAB, Math Works). Filter settings were optimized visually to obtain the maximal resolution of wave shape, as well as the least intrusion of fast (e.g., spindle) activities (6–8). Slow waves were detected as negative deflections of the EEG signal between two consecutive positive deflections below the zero crossing separated by at least 0.1 s. The peak-to-peak amplitude of the first and second segment of the wave and the slopes (mean first derivative of the first and second segment) were computed for each individual wave during NREM sleep.

To investigate spontaneous traveling waves, large slow waves (>median amplitude) were detected in each of the three derivations (either frontal, parietal, or occipital = "origin" derivation). The slow wave negative peak in the origin was used as reference, and the slow wave was considered to be propagating if (1) a negative peak in the other two derivations occurred within the following 50–200 ms and (2) the corresponding waves were at least 1/5 of the amplitude of the origin wave (7).

Baseline Sleep on the DOW. Visual observations and quantitative analysis revealed that all rats were well adapted to the DOW before the experiment began, with no abnormalities in their behavior and sleep/wake cycle (mean values in hours ± SD: light period, wake: 4.86 ±1.24, NREM sleep: 5.53 ± 0.89, REM sleep: 1.21 ± 0.42; dark period, wake: 8.43 ± 0.86, NREM sleep: 2.63 ± 0.42 h, REM sleep: 0.38 ± 0.14; light vs. dark, $P < 0.01$ for all three vigilance states). Measures of sleep architecture (e.g., duration and frequency of sleep episodes, number and distribution of brief awakenings, see Figs. 1*D*and 5*A*), and NREM SWA profile (Fig. S1 *A* and *B*) were also similar to those reported in rats recorded in their home cages (5, 9).

The frontal, parietal, and occipital derivations showed previously reported regional EEG differences during wake and sleep (9, 10): total EEG power was higher in the frontal and parietal derivations as compared with the occipital derivation, with the exception of the theta frequency band in wake and REM sleep (Fig. S1*C*). In NREM sleep EEG power in SWA (0.5–4.0 Hz) and spindle range (10–15 Hz) was greater in frontal than in posterior regions (Fig. S1*C*). The homeostatic changes of NREM SWA also exhibited the previously described frontal predominance (10, 11) frontal vs. parietal, 141.7 ± 5.4 vs. 136.0 ± 4.3, % of mean 24-h BSL, $P < 0.01$).

To investigate whether the changes of SWA during baseline were homeostatic, e.g., directly related to the sleep/wake history, we first computed the amount of SWA after spontaneously occurring wake episodes >10 min. As previously reported in mice (12), longer wake episodes were consistently followed by more intense and consolidated sleep, irrespective of time of day (Fig. S1 *D* and *E*). Moreover, wake episodes with only few sleep attempts were followed by significantly increased NREM SWA, whereas SWA did not increase after wake episodes containing >5% of NREM sleep (Fig. S1*F*). Finally, we found that intense sleep, characterized by high values of SWA, was more effective in dissipating sleep pressure: thus, the extent of the SWA decrease from one 2-h interval to the next was predicted by the value of SWA during the first interval (Fig. S1*G*).

1. Rechtschaffen A, Bergmann BM, Gilliland MA, Bauer K (1999) Effects of method, duration, and sleep stage on rebounds from sleep deprivation in the rat. *Sleep* 22: 11–31.
2. Trachsel L, Tobler I, Achermann P, Borbély AA (1991) Sleep continuity and the REM-nonREM cycle in the rat under baseline conditions and after sleep deprivation. *Physiol Behav* 49:575–580.
3. Trachsel L, Tobler I, Borbély AA (1986) Sleep regulation in rats: Effects of sleep deprivation, light, and circadian phase. *Am J Physiol* 251:R1037–R1044.
4. Vyazovskiy VV, Achermann P, Tobler I (2007) Sleep homeostasis in the rat in the light and dark period. *Brain Res Bull* 74:37–44.
5. Franken P, Dijk DJ, Tobler I, Borbély AA (1991) Sleep deprivation in rats: Effects on EEG power spectra, vigilance states, and cortical temperature. *Am J Physiol* 261: R198–R208.
6. Achermann P, Borbély AA (1997) Low-frequency (< 1 Hz) oscillations in the human sleep electroencephalogram. *Neuroscience* 81:213–222.
7. Vyazovskiy VV, Faraguna U, Cirelli C, Tononi G (2009) Triggering slow waves during NREM sleep in the rat by intracortical electrical stimulation: Effects of sleep/wake history and background activity. *J Neurophysiol* 101:1921–1931.
8. Vyazovskiy VV, Riedner BA, Cirelli C, Tononi G (2007) Sleep homeostasis and cortical synchronization: II. A local field potential study of sleep slow waves in the rat. *Sleep* 30:1631–1642.
9. Vyazovskiy VV, Borbély AA, Tobler I (2002) Interhemispheric sleep EEG asymmetry in the rat is enhanced by sleep deprivation. *J Neurophysiol* 88:2280–2286.
10. Huber R, Deboer T, Tobler I (2000) Topography of EEG dynamics after sleep deprivation in mice. *J Neurophysiol* 84:1888–1893.
11. Vyazovskiy VV, Ruijgrok G, Deboer T, Tobler I (2006) Running wheel accessibility affects the regional electroencephalogram during sleep in mice. *Cereb Cortex* 16: 328–336.
12. Huber R, Deboer T, Tobler I (2000) Effects of sleep deprivation on sleep and sleep EEG in three mouse strains: Empirical data and simulations. *Brain Res* 857:8–19.

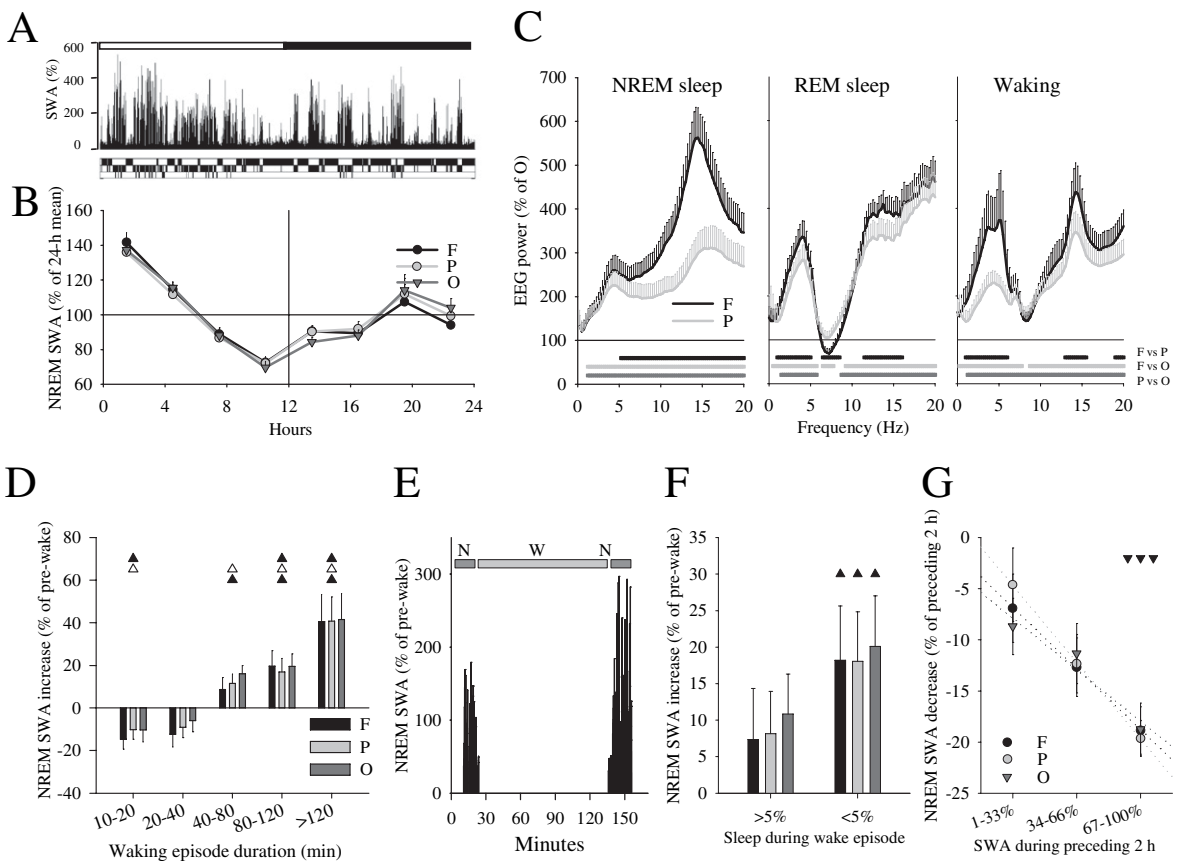

Fig. S1. (*A*) SWA (percentage of 24-h mean value in NREM sleep) and hypnogram of the 24-h baseline in one individual rat. Note high values of SWA at the beginning of the light period. (*B*) Time course of NREM SWA in the frontal (F), parietal (P), and occipital (O) cortex during baseline. Mean values ± SEM, $n = 11$. (*C*) Baseline EEG power spectra in the frontal and parietal derivation expressed as percentage of the EEG spectrum in the occipital derivation. Mean values ± SEM, $n = 8$. Horizontal lines below the curves depict frequency bins where EEG power differed significantly across derivations ($P < 0.05$, paired t test). (*D*) Effects of spontaneous wake episode duration (>10 min) on NREM SWA. Bars show the change of SWA (30-min intervals consisting of at least 33% of NREM sleep before and after wake episodes) from prewake levels. Mean values ± SEM, $n = 11$. Triangles depict significant changes ($P < 0.05$, paired t test). (*E*) Typical example of the increase in NREM SWA after a long spontaneous wake episode. (*F*) Change in NREM SWA in the frontal derivation after spontaneous wake episodes (mean values ± SEM, $n = 11$ rats). All wake episodes were subdivided into those with short sleep intrusions (>5% sleep) and those containing <5% of NREM sleep. Triangles depict significant differences from prewake levels (*G*). Decrease of NREM SWA from one 2-h interval to the next as a function of the level of SWA during the first interval (mean values ± SEM, $n = 8$).

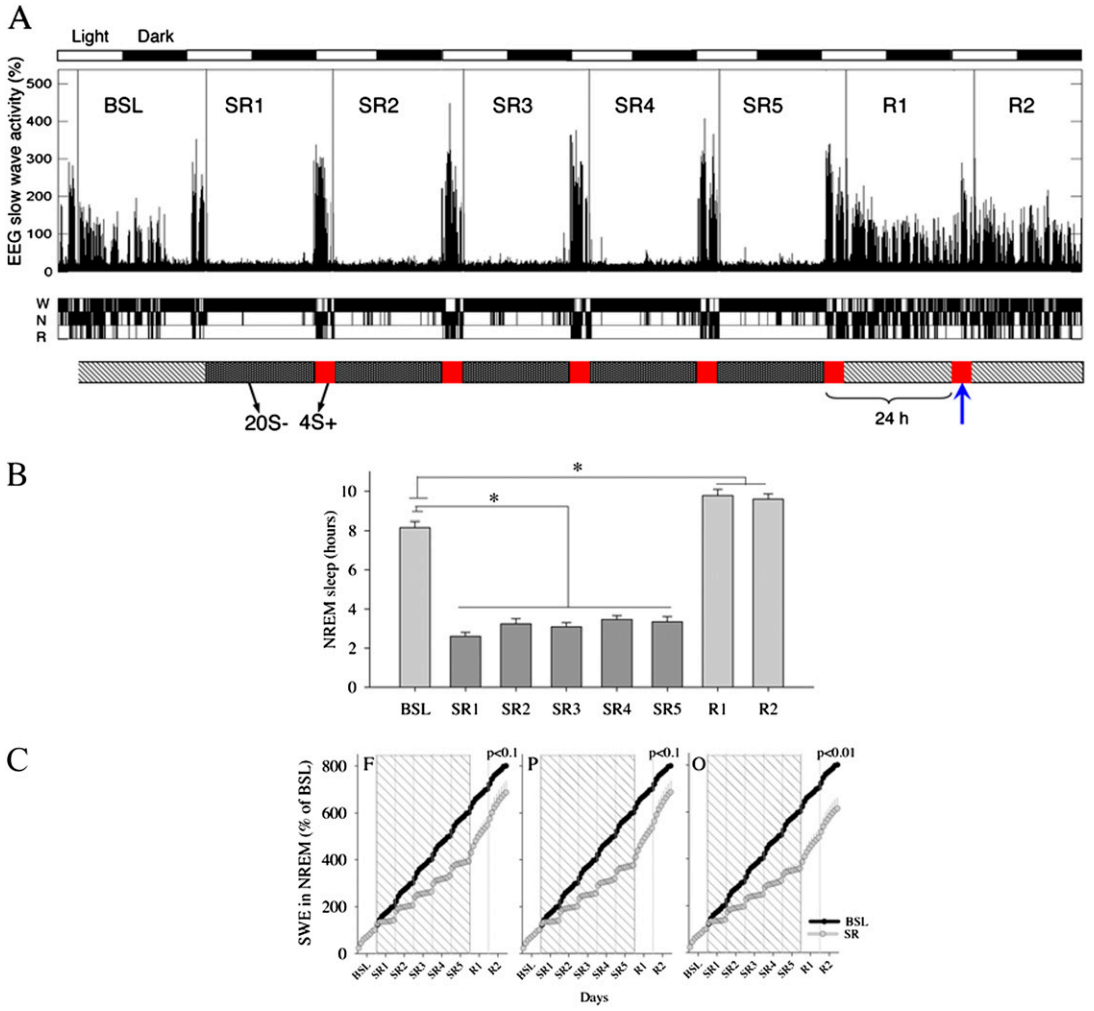

Fig. S2. (*A*) Schematic of the experimental design: the SR experiment starts with the 20S^{-} period, 4 h after lights on, followed by the 4S^{+} (red block), which therefore occurs during the following light period. Note that the R1 red block (blue arrow) occurs after rats had already slept ad libitum for 24 h. (*B*) Amount of NREM sleep during 24 h (mean ± SEM, $n = 11$). Asterisks indicate differences relative to the first SR day [$P < 0.05$, paired t test after significance in rANOVA, factor "day": $F(7,70) = 202.3$; $P < 0.0001$]. (*C*) Time course of total (cumulative) SWE in NREM sleep during baseline, SR (shaded area) and 2 recovery days. Mean values, $n = 8$.

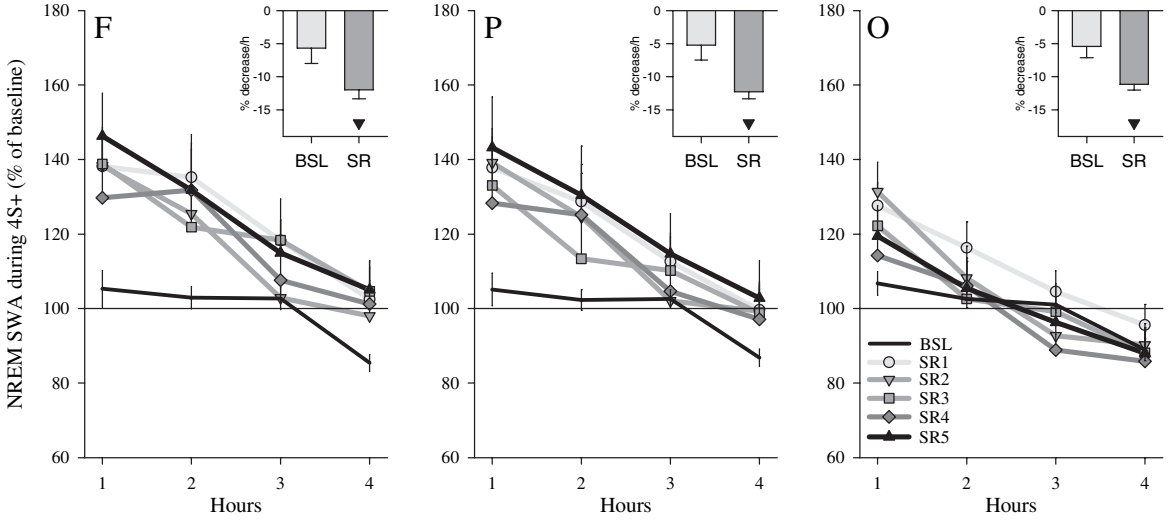

Fig. S3. Time course of SWA in NREM sleep during the 4S^{+} periods during baseline (BSL) and 5 consecutive days of sleep restriction (SR1-5) in the frontal (F), parietal (P), and occipital (O) derivations. Mean hourly values (SEM), $n = 8$. *Insets*: the rate of decline of SWA (% per 1 h) for BSL and SR days. Mean values (SEM), $n = 8$. Triangles: significant difference from baseline ($P < 0.05$, paired t test).

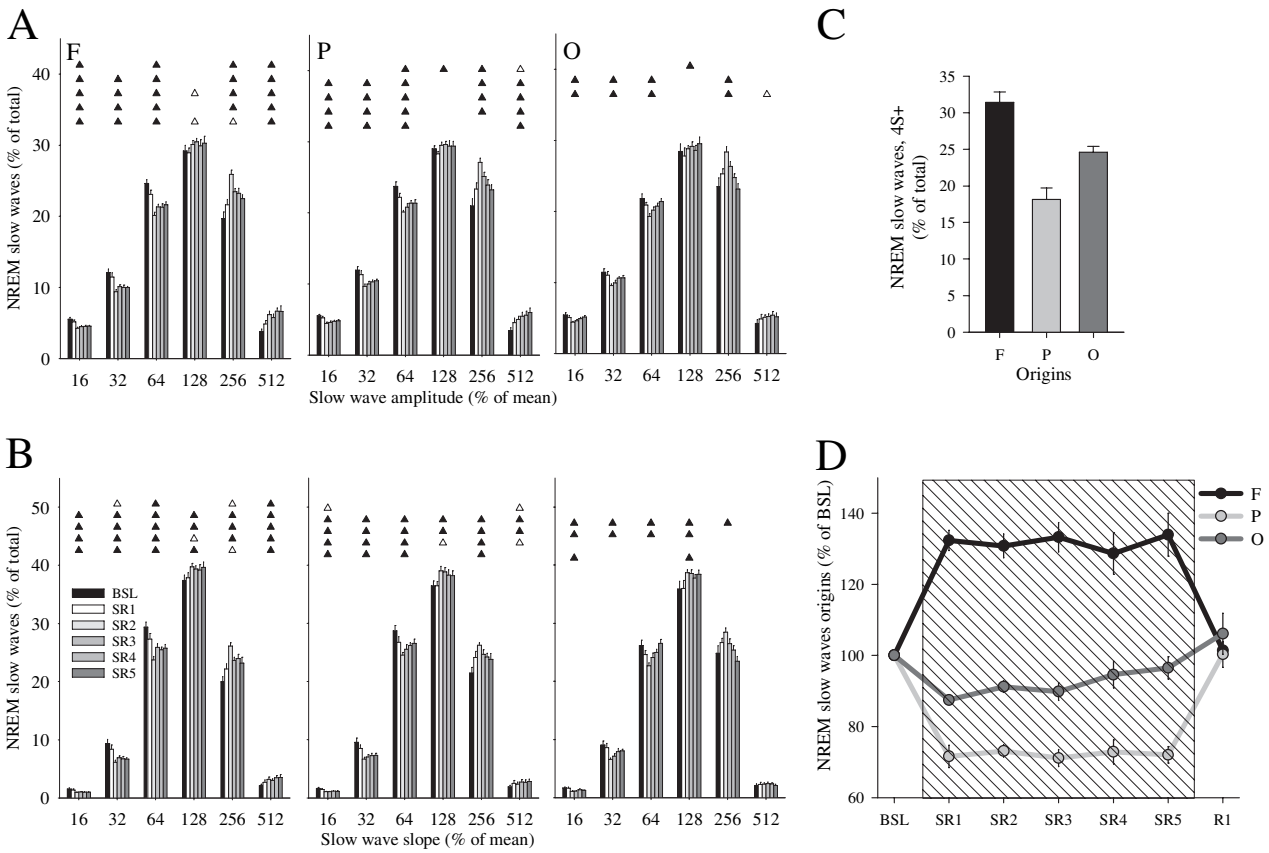

Fig. S4. Histogram of the distribution of NREM sleep slow waves during the 4S$^+$ periods as a function of their amplitude (*A*) or slope (*B*). The number of slow waves was computed within logarithmically increasing amplitude or slope ranges (% of mean amplitude or slope over all slow waves: 0–16, 17–32, 33–64, 65–128, 129–256, and 257–512%) and plotted against the upper boundary of the corresponding range. Triangles: differences from BSL (black, $P < 0.05$; white, $P < 0.1$). (*C*) Proportion of slow waves originating at different cortical locations. Mean values (±SEM, $n = 6$), expressed as percentage of all slow waves. (*D*) Number of NREM slow waves originating from the frontal, parietal, or occipital location during the 5 d of SR and recovery (R), plotted as percentage of the corresponding baseline value (BSL; mean values ± SEM, $n = 6$).

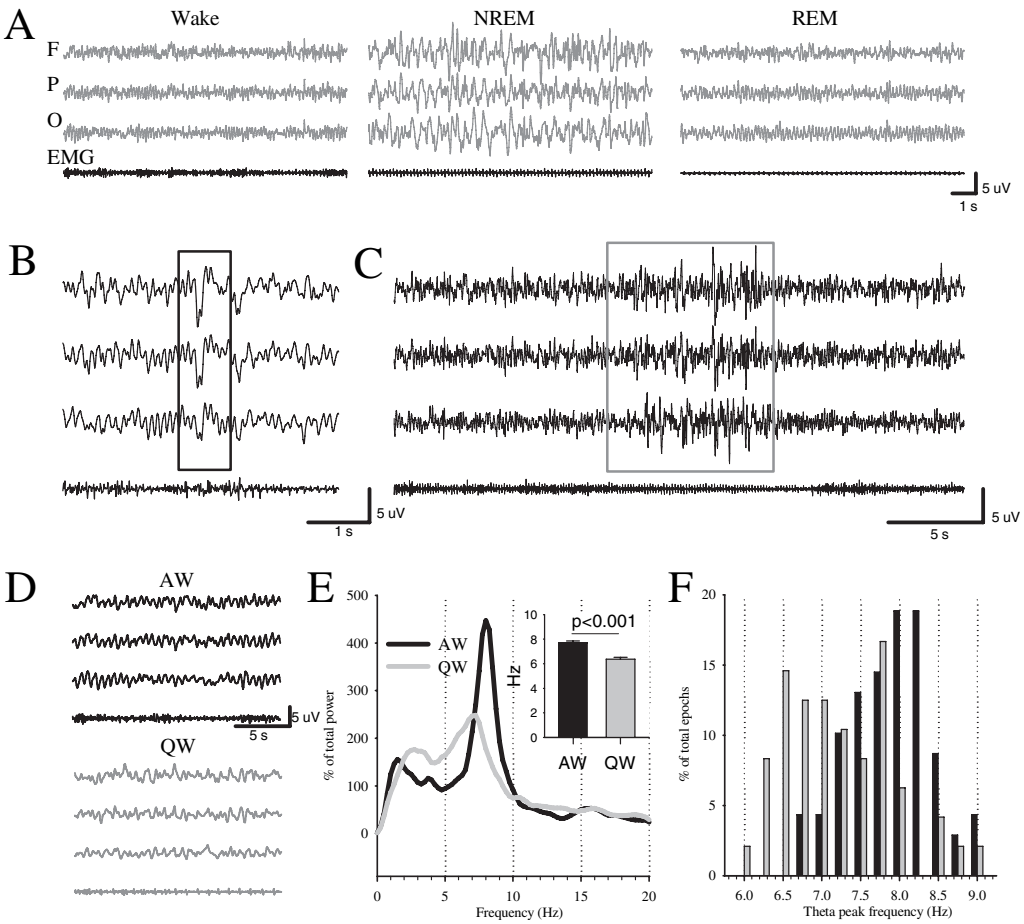

Fig. S5. (*A*) 12-s EEG traces from frontal (F), parietal (P), and occipital (O) cortex and corresponding electromyogram (EMG) in a representative rat during baseline in wake, NREM sleep, and REM sleep. (*B*) Isolated slow wave during 20S^{-}. (*C*) A 30-s recording depicting a typical example of sleep attempt during 20S^{-}: EMG decreases while large slow waves appear in all three derivations. (*D*) Typical examples of EEG and EMG (*Bottom* trace) recordings in active waking (AW) and quiet waking (QW): AW is characterized by regular theta activity and high EMG, whereas QW is dominated by a slower EEG pattern and reduced muscle tone. (*E*) EEG power spectra in AW and QW (~5 min per state) during baseline. *Inset* depicts mean frequency of the theta peak (±SEM). (*F*). Histogram of the distribution of 4-s epochs in AW and QW as a function of the frequency of the theta peak.

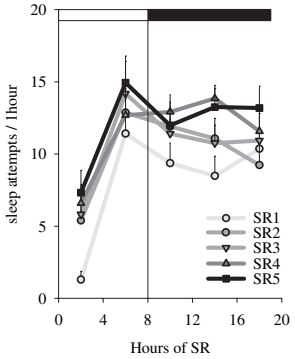

Fig. S6. Time course of the occurrence of sleep attempts (≤16 s) during the 20S^{-} periods. Mean 3-h values (SEM), n = 11.

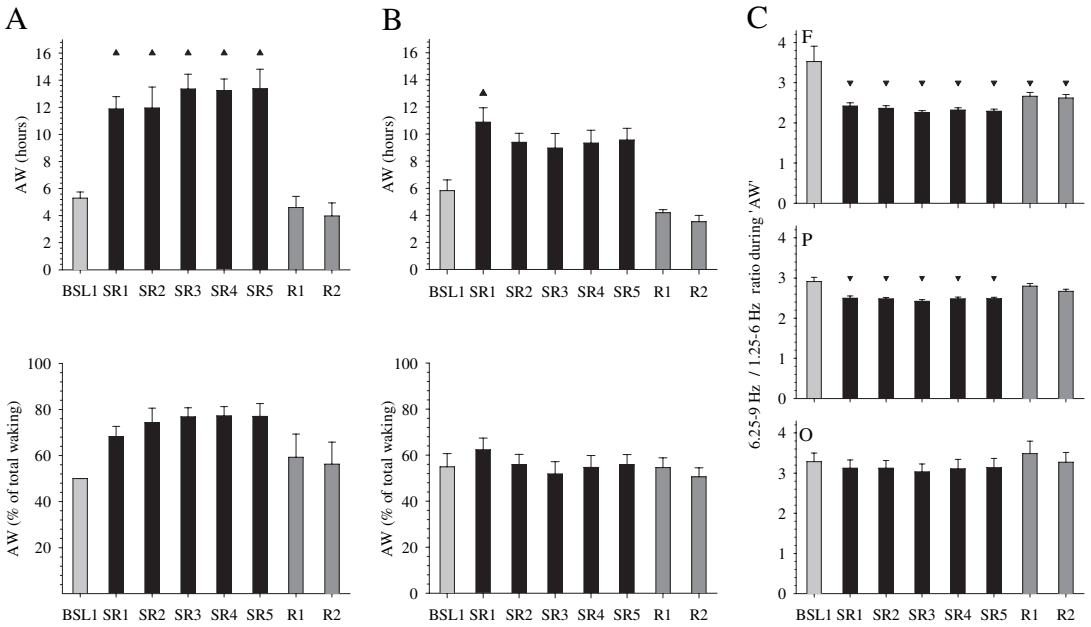

Fig. S7. Effect of disk rotation on the amount of active wake (AW). (*A*) Amount of AW defined based on the EMG variance: all epochs in which the EMG variance was greater than the median EMG variance during baseline wake were considered AW (waking with high locomotor activity; the remaining epochs were then QW or wake with low locomotor activity). Baseline (BSL), 5 SR days (SR1-5) and 2 d of recovery (R1-2) are shown. Mean values + SEM, $n = 6$. By definition, during baseline 50% of waking is AW. Note that the absolute (total in 24 h) amount of AW is significantly higher on SR days (*Upper*), but the relative amount (% of total wake) is not significantly different between days (*Lower*, triangles: $P < 0.05$, Dunn-Sidak test). (*B*) Amount of AW defined based on theta EEG power, which was required to be at least 50% higher than the low frequency EEG power (6.25–9 Hz/1.25–6 Hz > 1.5). Mean values ± SEM, $n = 6$. The total amount of AW was significantly different from baseline on the first SR day (triangle, $P < 0.05$, Dunn-Sidak test). The relative amount of AW (% of total wake) was not significantly different from baseline. There was high correlation between the amount of AW defined as high EMG and AW defined on the basis of theta activity ($r = 0.68$; $P < 0.001$, Pearson correlation). (*C*) Mean 6.25–9 Hz/1.25–6 Hz ratio in AW (e.g., epochs with ratio > 1.5) during baseline (BSL), 5 SR d (SR1-5), and 2 d of recovery (R1-2) for the frontal (F), parietal (P), and occipital (O) derivation. Mean values + SEM, $n = 8$. Triangles depict days where the ratio was significantly different from baseline (triangles, $P < 0.05$, Dunn-Sidak test).

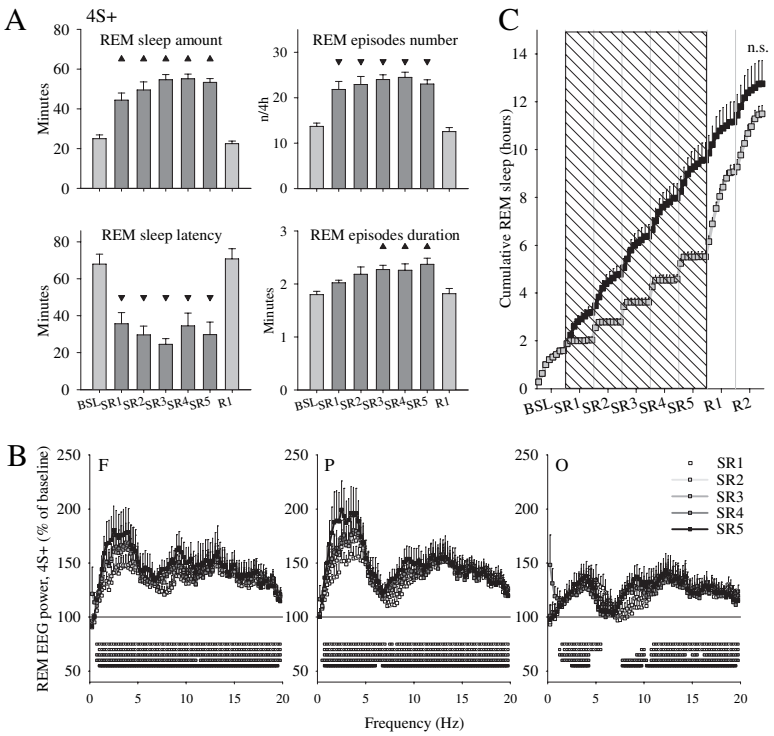

Fig. S8. (*A*) Mean values (±SEM, $n = 11$) of REM sleep amount, REM sleep latency, REM episodes' number and duration during the first 4 h after light onset during baseline (BSL), 5 d of SR ($4S^+$ intervals), and the first day of recovery (R1). Triangles depict significant differences from BSL ($P < 0.05$ after Bonferroni correction, mean ± SEM, $n = 11$). (*B*) REM sleep EEG power during $4S^+$ in the 5 d of SR plotted as percentage of the corresponding baseline period (mean ± SEM, $n = 8$). Squares depict frequency bins that differed significantly from baseline ($P < 0.05$, paired t test). (*C*) Cumulative time course of REM sleep during baseline and SR (shaded area). (SEM, $n = 8$). Note that the error bars for the baseline curves increase cumulatively due to the large interindividual variability during the first 24 h of baseline.